Synthesis, Structure, and Redox Reactivity of a Substituted Niobocene Formaldehyde Complex. Importance of Hydrogen Bonding in the Redox Chemistry

B. Thiyagarajan,[1a] Lucyna Michalczyk,[1a] John C. Bollinger,[1b] John C. Huffman,[1b] and Joseph W. Bruno*,[1a]

Department of Chemistry, Wesleyan University, Middletown, Connecticut 06459, and Molecular Structure Center, Indiana University, Bloomington, Indiana 47405

Received February 13, 1996[⊗]

The niobocene chloride $[Cp'_2Nb(\mu\text{-}Cl)]_2$ (**1**, $Cp' = \eta^5\text{-}C_5H_4SiMe_3$) reacts with a suspension of paraformaldehyde to yield an η^2-formaldehyde complex $Cp'_2Nb(Cl)(\eta^2\text{-}CH_2O)$ (**2**), the crystal structure of which was determined by X-ray diffraction. This compound undergoes facile reduction with sodium amalgam to produce the Nb(IV) radical $Cp'_2Nb(\eta^2\text{-}CH_2O)$ (**3**); the latter is unstable toward isolation but was found stable in dilute solution and characterized with ESR and infrared techniques. If a similar reduction of **2** is carried out in the presence of added alcohol, the result is instead the diamagnetic hydride $Cp'_2Nb(H)(\eta^2\text{-}CH_2O)$ (**4**); the process thus constitutes a sodium/ethanol reduction used to convert a halide to a hydride. Radical **3** was confirmed to reside on the path to **4**, and **3** is only susceptible to subsequent reduction if alcohol is present. This has been attributed to hydrogen-bond activation, and the reduction of the resulting intermediate (**5**) was observed in voltammetric studies.

Introduction

The longstanding interest in the chemistry of transition metal formaldehyde complexes is largely derived from suggestions that surface-bound formaldehyde may be involved in metal-catalyzed reduction of carbon monoxide. Proposed mechanisms involve a sequence of formyl, formaldehyde, hydroxymethyl, and methylene on the path to methanol,[2] and formaldehyde complexes have also been implicated in C−C bond-forming reactions leading to glycol derivatives.[3] Other ketones and aldehydes also complex with molecular metal systems,[4−18] and have been shown to exhibit isomerization processes involving η^1-O (**A**) and η^2-C,O (**B**) isomers;[4,15,16] many

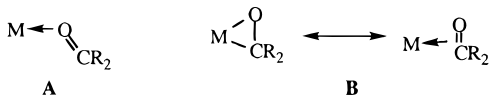

of these have been utilized effectively in metal-induced enantioselective additions of nucleophiles,[4c−g] and these reactions typically involve the reactive η^1-O isomer. However, formaldehyde is invariably observed to adopt the η^2-C,O binding mode, and this has been attributed to a combination of favorable steric interactions (lack of aldehyde substituent) and the low energy of the formaldehyde π^* acceptor orbital;[4e] this energy is low relative to that of other carbonyl π^* orbitals and matches well with the energy of the metal donor orbital.

Viable synthetic routes to aldehyde and ketone complexes include (a) direct reaction of an unsaturated metal complex or precursor with the carbonyl,[4,6,7,9−13,15−18]

⊗ Abstract published in *Advance ACS Abstracts,* March 15, 1996.

(1) (a) Wesleyan University. (b) Indiana University.

(2) (a) Henrici-Olivé, G.; Olivé, S. *Angew. Chem., Int. Ed. Engl.* **1976**, *15*, 136−141. (b) Numan, J. G.; Bogdan, C. E.; Klier, K.; Smith, K. J.; Young, C.-W.; Herman, R. G. *J. Catal.* **1988**, *113*, 410−433. (c) Mitchell, W. J.; Xie, J.; Jachimowski, T. A.; Weinberg, W. H. *J. Am. Chem. Soc.* **1995**, *117*, 2606−2617.

(3) (a) Dombek, B. D.; *J. Am. Chem. Soc.* **1980**, *102*, 6855−6857. (b) Dombek, B. D. *J. Chem. Educ.* **1986**, *63*, 210−212. (c) Ishino, M.; Tamura, M.; Deguchi, T.; Nakamura, S. *J. Catal.* **1987**, *105*, 478−482. (d) Wolczanski, P. T.; Bercaw, J. E. *Acc. Chem. Res.* **1980**, *13*, 121−127. (e) Maatta, E. A.; Marks, T. J. *J. Am. Chem. Soc.* **1983**, *103*, 3576−3578.

(4) (a) Huang, Y.-H.; Gladysz, J. A. *J. Chem. Educ.* **1988**, *65*, 298−303. (b) Agbossou, F.; Ramsden, J. A.; Yo-Hsin, H.; Arif, A. M.; Gladysz, J. A. *Organometallics* **1982**, *11*, 692−701. (c) Klein, D. P.; Gladysz, J. A. *J. Am. Chem. Soc.* **1991**, *114*, 8710−8711. (d) Méndez, N. Q.; Seyler, J. W.; Arif, A. M.; Gladysz, J. A. *J. Am. Chem. Soc.* **1993**, *115*, 2323−2334. (e) Garner, C. M.; Mendez, N. Q.; Kowalczyk, J. J.; Fernandez, J. M.; Emerson, K.; Larsen, K. D.; Gladysz, J. A. *J. Am. Chem. Soc.* **1990**, *112*, 5146−5160. (f) Méndez, N. Q.; Arif, A. M.; Gladysz, J. A. *Angew. Chem., Int. Ed. Engl.* **1990**, *29*, 1473−1474. (g) Méndez, N. Q.; Mayne, C. L.; Gladysz, J. A. *Angew. Chem., Int. Ed. Engl.* **1990**, *29*, 1475−1476.

(5) Brown, K. L.; Clark, G. R.; Headford, C. E. L.; Marsden, K.; Roper, W. R. *J. Am. Chem. Soc.* **1979**, *101*, 503−505.

(6) (a) Gambarotta, S.; Floriani, C.; Chiesi-Villa, A.; Guastini, C. *J. Am. Chem. Soc.* **1983**, *105*, 1690−1691. (b) Gambarotta, S.; Floriani, C.; Chiesi-Villa, A.; Guastini, C. *J. Am. Chem. Soc.* **1982**, *104*, 2019−2020. (c) Gambarotta, S.; Floriani, C.; Chiesi-Villa, A.; Guastini, C. *Organometallics* **1986**, *5*, 2425−2433.

(7) Herberich, G. E.; Okuda, J. *Angew. Chem., Int. Ed. Engl.* **1985**, *24*, 402.

(8) Erker, G.; Kropp, K.; Krüger, C.; Chiang, A.-P. *Chem. Ber.* **1982**, *115*, 2447−2460.

(9) (a) Berke, H.; Bankhardt, W.; Huttner, G.; v. Seyerl, J.; Zsolnai, L. *Chem. Ber.* **1981**, *114*, 2754−2768. (b) Berke, H.; Huttner, G.; Weiler, G.; Zsolnai, L. *J. Organomet. Chem.* **1981**, *219*, 353−362.

(10) (a) Faller, J. W.; Ma, Y.; Smart, C. J.; DiVerdi, M. J. *J. Organomet. Chem.* **1991**, *420*, 227−252. (b) Faller, J. W.; Ma, Y. *J. Am. Chem. Soc.* **1991**, *113*, 1579−1586.

(11) Banchard, B.; Wuest, J. D. *Organometallics* **1991**, *10*, 2015−2025.

(12) Hill, J. E.; Fanwick, P. E.; Rothwell, I. P. *Organometallics* **1992**, *11*, 1771−1773.

(13) Bochmann, M.; Webb, K. J.; Hursthouse, M. B.; Mazid, M. *J. Chem. Soc., Chem. Commun.* **1991**, 1735−1737.

(14) Adams, H.; Bailey, N. A.; Gautlett, J. T.; Winter, M. J.; Woodward, S. *J. Chem. Soc., Dalton Trans.* **1991**, 2217−2221.

(15) Powell, D. W.; Lay, P. A. *Inorg. Chem.* **1991**, *31*, 3542−3550.

(16) (a) Harman, W. D.; Dobson, J. C.; Taube, H. *J. Am. Chem. Soc.* **1989**, *111*, 3061−3062. (b) Harman, W. D.; Sekine, M.; Taube, H. *J. Am. Chem. Soc.* **1988**, *110*, 2439−2445.

(17) Rabinovich, D.; Parkin, G. *J. Am. Chem. Soc.* **1991**, *113*, 5904−5905.

(18) Bullock, R. M.; Rappoli, B. J. *J. Am. Chem. Soc.* **1991**, *113*, 1659−1669.

0276-7333/96/2315-1989$12.00/0

(b) reaction of metal alkylidene with an oxygen atom source,[19] (c) reduction of carbon monoxide by appropriate metal hydrides,[6a,8] and (d) β-hydride elimination by alkoxide complexes to give hydridocarbonyl complexes (eq 1).[20−37] The first of these has been most frequently

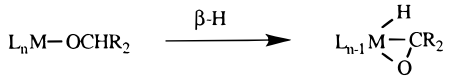

(1)

applied, and its use in the synthesis of formaldehyde complexes has been aided by the realization that solid paraformaldehyde can serve as a useful source of the desired ligand. We[38] and others[39] have been pursuing the chemistry of the bent metallocene fragment Cp'_2NbCl ($Cp' = \eta^5$-$C_5H_4SiMe_3$), which has been shown recently to adopt the dimeric strucuture $[Cp'_2Nb(\mu\text{-}Cl)]_2$ (**1**) in the solid state.[39e] The monomeric fragment has proven to be extremely electron rich, and we have reported on the mechanism of its facile aerobic oxidation.[38f] The compound also functions as an effective π donor, forming stable complexes with linear π acceptor ligands such as carbon monoxide and isocyanides;[39] indeed, the carbonyl adduct $Cp'_2Nb(Cl)(CO)$ shows evidence of a considerable back-bonding component, with a C−O stretching frequency (1930 cm^{-1}) at relatively low energy. Acceptor ligands with sp-hybridized carbon, e.g., alkynes[39a] and heterocumulenes,[38,39] also exhibit strong side-on binding to the niobocene center. Interestingly, however, this metal fragment shows relatively little tendency to form stable complexes with alkenes, carbonyls ($R_2C{=}O$), or other sp^2 carbon-containing ligands (although a styrene complex has been reported recently);[39i] in this sense it differs from the closely related C_5H_5 and C_5Me_5 niobium derivatives, as well as from a number of closely related early transition metal complexes.

In the work described herein, we undertook a study of the chemistry of **1** with formaldehyde. We sought to prepare the adduct, to determine its susceptibility to redox chemistry, and to seek methods to replace the chloride coligand with other coligands. In the course of this we have utilized a combination of sodium metal and alcohol to introduce a hydride ligand; we previously reported the use of a related reaction in the conversion of analogous ketene complexes $Cp'_2Nb(Cl)(\eta^2\text{-}O{=}C{=}CR_2)$ to the hydride derivatives $Cp'_2Nb(H)(\eta^2\text{-}O{=}C{=}CR_2)$.[38e] In the ketene case, we presented evidence for ketene ligand involvement and the intermediacy of an acyl derived from reduction and protonation of the ketene. A related process with a formaldehyde ligand could involve the intermediacy of an alkoxide, as in route d above (eq 1); we thus initiated a mechanistic study on the use of this reaction for converting metal chloride to metal hydride. We report here the results of synthetic, structural, and mechanistic studies indicating that the formaldehyde ligand facilitates the process in another manner, by using the oxygen to support a hydrogen-bonded complex prior to the final redox event.

Experimental Section

General Considerations. All manipulations involving metal complexes were carried out under an atmosphere of nitrogen which was first passed through activated BTS catalyst and molecular sieves. Standard Schlenk techniques were used to handle solutions,[40] and solids were transferred in a Vacuum Atmospheres Corp. glovebox under purified nitrogen. Solvents toluene, hexane, and tetrahydrofuran (J. T. Baker) were distilled from sodium benzophenone ketyl under nitrogen. $NbCl_5$ and paraformaldehyde (Aldrich) were commercial materials; the latter was dried in vacuo prior to use.

NMR spectra were obtained on a Varian Gemini 300 FT-NMR instrument, infrared spectra on a Perkin-Elmer Model 1600 FT-IR spectrophotometer, ESR spectra on a Bruker ESP300 spectrometer, and voltammetric data with an EG&G VersaStat potentiostat interfaced to a 486 PC. The electrolytic cell was evacuated on a Schlenk line and then loaded with a solution of 0.5 M $NBu_4^+PF_6^-$ in THF. The reference electrode was prepared by inserting a short (ca. $^1/_4$ in.) length of 5 mm

(19) Buhro, W. E.; Georgiou, S.; Fernandez, J. M.; Patton, A. T.; Strouse, C. E.; Gladysz, J. A. *Organometallics* **1985**, *5*, 956−965.
(20) Van Asselt, A.; Burger, B. J.; Gibson, V. C.; Bercaw, J. E. *J. Am. Chem. Soc.* **1986**, *108*, 5347−5349.
(21) Green, M. L. H.; Parkin, G.; Moynihan, K. J.; Prout, K. *J. Chem. Soc., Chem. Commun.* **1984**, 1540−1541.
(22) Hoffman, D. M.; Lappas, D.: Wierda, D. A. *J. Am. Chem. Soc.* **1993**, *115*, 10538−10544.
(23) (a) Ovalles, C.; Fernandez, C.; Darensbourg, D. J. *J. Mol. Catal.* **1994**, *93*, 125−136. (b) Darensbourg, D. J.; Ovalles, C. *J. Am. Chem. Soc.* **1987**, *109*, 3330−3336.
(24) Bernard, K. D.; Rees, W. M.; Atwood, J. D. *Organometallics* **1986**, *5*, 390−391.
(25) Bryndza, H. E.; Calabrese, J. C.; Marsi, M.; Roe, D. C.; Tam, W.; Bercaw, J. E. *J. Am. Chem. Soc.* **1986**, *108*, 4805−4813.
(26) Saura-Llamas, I.; Gladysz, J. A. *J. Am. Chem. Soc.* **1992**, *114*, 2136−2144.
(27) Chatt, J.; Shaw, B. L.; Field, A. E. *J. Chem. Soc.* **1964**, 3466−3475.
(28) Whitesides, G. M.; Sadowski, J. S.; Lilburn, J. *J. Am. Chem. Soc.* **1974**, *96*, 2829−2835.
(29) Kölle, U.; Kang, B.-S.; Raabe, G.; Krüger, C. *J. Organomet. Chem.* **1990**, *386*, 261−266.
(30) Nugent, W. A.; Zubyk, R. M. *Inorg. Chem.* **1986**, *25*, 4604−4606.
(31) Sasson, Y.; Blum, J. *J. Chem. Soc., Chem. Commun.* **1974**, 309−310.
(32) Chaudret, B. N.; Cole-Hamilton, D. J.; Nohr, R. S.; Wilkinson, G. *J. Chem. Soc., Dalton Trans.* **1977**, 1546−1547.
(33) Gaus, P. L.; Jones, L. M.; Zamiska, L. A. *Polyhedron* **1989**, *8*, 653−657.
(34) Bruno, J. W.; Huffman, J. C.; Caulton, K. G. *Inorg. Chim. Acta* **1984**, *89*, 167−173.
(35) Schalley, C. A.; Wesendrup, R.; Schroder, D.; Weiske, T.; Schwarz, H. *J. Am. Chem. Soc.* **1995**, *117*, 7711−7718.
(36) (a) Blum, O.; Milstein, D. *J. Am. Chem. Soc.* **1995**, *117*, 4582−4594. (b) Blum, O.; Milstein, D. *Angew. Chem., Int. Ed. Engl.* **1995**, *34*, 229−231.
(37) Barry, J. T.; Chacon, S. T.; Chisholm, M. H.; Huffman, J. C.; Streib, W. E. *J. Am. Chem. Soc.* **1995**, *117*, 1974−1990.
(38) (a) Halfon, S. E.; Fermin, M. C.; Bruno, J. W. *J. Am. Chem. Soc.* **1989**, *111*, 5490−5491. (b) Bruno, J. W.; Fermin, M. C.; Halfon, S. E.; Schulte, G. K. *J. Am. Chem. Soc.* **1989**, *111*, 8738−8740. (c) Fermin, M. C.; Bruno, J. W. *J. Am. Chem. Soc.* **1993**, *115*, 7511−7512. (d) Fermin, M. C.; Bruno, J. W. *Tetrahedron Lett.* **1993**, *34*, 7545−7548. (e) Fermin, M. C.; Hneihen, A. S.; Maas, J. J.; Bruno, J. W. *Organometallics* **1993**, *12*, 1845−1856. (f) Thiyagarajan, B.; Kerr, M. E.; Bruno, J. W. *Inorg. Chem.* **1995**, *34*, 3444−3452. (g) Fermin, M. C.; Thiyagarajan, B.; Bruno, J. W. *J. Am. Chem. Soc.* **1993**, *115*, 974−979.
(39) (a) Añtinolo, A.; Gomez-Sal, P.; de Llarduya, J. M.; Otero, A.; Royo, P.; Carrerra, S. M.; Blanco, S. G. *J. Chem. Soc., Dalton Trans.* **1987**, 975−980. (b) Martinez de Ilarduya, J. M.; Otero, A.; Royo, P. *J. Organomet. Chem.* **1988**, *340*, 187−193. (c) Antinolo, A.; Fajardo, M.; Mardomingo, C. L.; Otero, A.; Mourad, Y.; Munier, Y.; Sanz-Aparicio, J.; Fonseca, I.; Florencio, F. *Organometallics*, **1990**, *9*, 2919−2925. (d) Antinolo, A.; Fajardo, M.; Mardomingo, C. L.; Martin-Villa, P.; Otero, A. *Organometallics* **1991**, *10*, 3435−3437. (e) Antiñolo, A.; Espinosa, P.; Fajardo, M.; Gomez-Sal, P.; Lopez-Mardomingo, C.; Martin-Alonso, A.; Otero, A. *J. Chem. Soc., Dalton Trans.* **1995**, 1007−1013. (f) Antiñolo, A.; de Llarduya, J. M.; Otero, A.; Royo, P.; Lanfredi, A. M. M.; Tiripicchio, A. *J. Chem. Soc., Dalton Trans.* **1988**, 2685−2693. (g) Antinolo, A.; Otero, A.; Fajardo, M.; Garcia-Yebra, C.; Gil-Sanz, R.; Lopez-Mardomingo, C.; Martin, A.; Gomez-Sal, P. *Organometallics* **1994**, *13*, 4679−4682. (h) Antinolo, A.; Fajardo, M.; Gil-Sanz, R.; Lopez-Mardomingo, C.; Otero, A. *Organometallics* **1994**, *13*, 1200−1207. (i) Antinolo, A.; Carillo, F.; Garcia-Yuste, S.; Otero, A. *Organometallics* **1994**, *13*, 2761−2766.
(40) Shriver, D. F.; Drezdzon, M. A. *The Manipulation of Air-Sensitive Compounds*; 2nd ed.; Wiley-Interscience: New York, 1986; Chapter 1.

porous vycor into a Teflon tube. The latter was filled with 0.1 M $AgNO_3/CH_3CN$ solution, into which a 16 gauge silver wire was immersed. The mercury-covered platinum working electrode was prepared as previously described.[41] The electrolytic solution was maintained under a nitrogen atmosphere by passing THF-saturated nitrogen through the cell.

(Trimethylsilyl)cyclopentadiene (Cp′H) was prepared using the literature method,[42a] with the exception that the THF solution of sodium cyclopentadienide was added in dropwise fashion to the Me_3SiCl solution; this ensures that the latter is always present in excess and minimizes the formation of disilyl byproducts. Cp′H was metalated with butyllithium and cyclopentadiene was metalated with sodium metal, both in THF. $NbCl_3(DME)$[42b] and $[Cp'_2NbCl]_2$ (**1**)[38e] were prepared using literature methods.

$Cp'_2Nb(Cl)(\eta^2\text{-}CH_2O)$ (2). Solid **1** (1.0 g, 2.48 mmol) and excess paraformaldehyde (2.5 g, 83 mmol) were weighed into a gas-inlet flask in the glovebox. On the Schlenk line, 50 mL of THF was added via syringe using a nitrogen purge. The resulting suspension was stirred for 24 h at ambient temperature and then filtered under nitrogen to remove excess paraformaldehdye. The solvent was removed in vacuo, and the solid residue was extracted with a minimum volume of hexanes. Cooling resulted in the precipitation of a light brown solid (0.85 g, 1.96 mmol, 79%). ^1H NMR (C_6D_6): 5.80 (2H, br[43] s, Cp′), 5.77 (2H, br s, Cp′), 5.37 (2H, br s, Cp′), 4.72 (2H, br s, Cp′), 3.37 (2H, s, CH_2), 0.21 ppm (18 H, s, $SiMe_3$). ^{13}C NMR (C_6D_6): 123.6, 117.5, 112.1, 106.8, 102.8 (Cp′), 67.8 (formaldehyde C), 0.08 ppm (SiMe). IR (Nujol): 1247 (s), 1178.5 (s, C−O stretch), 1159 (s), 1044 (vs), 902 (vs), 839 cm^{-1} (vs). Methyl derivative $Cp'_2Nb(Me)(\eta^2\text{-}CH_2O)$ was prepared similarly from known $Cp'_2Nb(Me)(PMe_3)$.[39a] ^1H NMR (C_6D_6): 5.45 (2H, br s, Cp′), 5.21 (2H, br s, Cp′), 5.16 (2H, br s, Cp′), 4.77 (2H, br s, Cp′), 3.00 (2H, s, CH_2), 0.85 (3H, s, Nb−Me), 0.27 (18H, s, SiMe). IR (Nujol): 1260 (s), 1177.2 (s, C−O stretch), 1148 (s), 1020 (vs), 905 (vs), 800 cm^{-1} (vs).

$Cp'Nb(H)(\eta^2\text{-}CH_2O)$ (4). Compound **2** (0.40 g, 0.92 mmol) and nitrogen-saturated methanol (0.5 mL, 12 mmol) were dissolved in 80 mL of toluene. This solution was added via syringe to a sodium amalgam containing 2.3 mmol of sodium in 2 mL of mercury. The resulting mixture was stirred for ca. 8 h to ensure complete reaction. The solution was removed from the amalgam with a syringe and then filtered through Celite under nitrogen. The solvent was removed in vacuo and the residue extracted with toluene. The toluene was evaporated and the product dissolved in a minimum volume of hexane; cooling (−78 °C) resulted in the precipitation of an off-white solid, which was filtered out and dried in vacuo (0.197 g, 0.49 mmol, 54%). ^1H NMR (C_6D_6): 5.50 (2H, br s, Cp′), 4.81 (2H, br s, Cp′), 4.57 (2H, br s, Cp′), 4.49 (2H, br s, Cp′), 2.30 (2H, s, CH_2O), 0.69 (1H, s, Nb−H), 0.32 ppm (18H, s, SiMe). ^{13}C NMR (C_6D_6): 108.9, 98.7, 97.7, 96.6, 92.1 (Cp′), 44.6 (formaldehyde C), 0.41 ppm (SiMe). IR (Nujol): 1697 (br w, Nb−H), 1171 (s, C−O stretch).

X-ray Crystallography. Compound **2** was crystallized by slowly cooling a toluene solution to −30 °C, resulting in pale yellow rods. A small crystal measuring 0.07 × 0.10 × 0.9 mm was transferred to the goniostat and cooled to −165 °C under a nitrogen atmosphere. A systematic search of reciprocal space located a set of data indicative of monoclininc symmetry and systematic absences corresponding uniquely to the centrosymmetric space group $P2_1/a$. Data were recorded using the moving crystal, moving detector technique with fixed background counts at each extreme of the scan. The data were corrected for Lorentz and polarization effects, and equivalent data were averaged. The structure was solved by direct methods (MULTAN) and Fourier techniques. Hydrogen atoms were located in a difference map phased on the non-hydrogen atoms and included as isotropic contributors in the final cycles of the least-squares fit.[44] The final model includes a disorder, according to which the chloride and formaldehyde positions are roughly interchanged (see Discussion) 9% of the time. A final difference Fourier map is featureless; the largest peak resides near the niobium atom and has an intensity of 0.56 e/Å^3. Data are collected in Tables 1 and 2.

Table 1. Crystallographic Data for 2

formula	$C_{17}H_{28}ClNbOSi_2$
fw	432.94
cryst dimens, mm	0.07 × 0.10 × 0.90
cell dimens (−165 °C, 64 reflcns)	
a, Å	14.671(2)
b, Å	6.857(1)
c, Å	20.459(2)
α, γ, deg	90
β, deg	108.64(1)
Z (molecules/cell)	
V, Å^3	1950.18
d(calcd), g cm^{-3}	1.475
wavelength, Å	0.710 69
linear abs coeff, cm^{-1}	8.492
R	0.404
R_w	0.0293

Table 2. Selected Bond Lengths (Å) and Angles (deg) for 2

Nb(1)−Cl(2)	2.5253(11)	Nb(1)−C(8)	2.435(4)
Nb(1)−O(3)	2.048(3)	Nb(1)−C(9)	2.437(4)
Nb(1)−C(4)	2.257(4)	Nb(1)−C(14)	2.424(4)
C(4)−O(3)	1.322(5)	Nb(1)−C(15)	2.407(4)
Nb(1)−C(5)	2.423(4)	Nb(1)−C(16)	2.454(4)
Nb(1)−C(6)	2.419(4)	Nb(1)−C(17)	2.452(4)
Nb(1)−C(7)	2.431(4)	Nb(1)−C(18)	2.441(4)
Cl(2)−Nb(1)−O(3)	77.32(9)	Nb(1)−C(4)−O(3)	63.65(19)
Cl(2)−Nb(1)−C(4)	112.67(10)	Nb(1)−O(3)−C(4)	80.99(22)
O(3)−Nb(1)−C(4)	35.36(13)		

Results

Preparation of Formaldehyde Complex 2. The niobocene compound **1** is a useful source of the monomer and is appreciably soluble in a variety of organic solvents. It was dissolved in THF and treated with an excess of solid paraformaldehyde. The resulting suspension was stirred for 24 h at ambient temperature, during which time a slow reaction (eq 2) leads to the

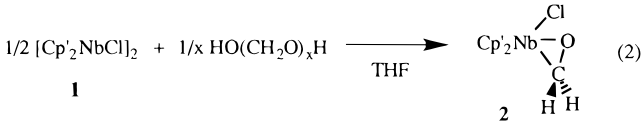

1 2 (2)

desired compound **2**; the latter is highly soluble in THF, and the solution was thus filtered to remove excess paraformaldehyde. Complex **2** was obtained as a light yellow-brown precipitate from hexane in ca. 80% yield and recrystallized from cold toluene. Alternatively, it may be prepared from monomeric precursors such as $Cp'_2Nb(Cl)(CO)$ or $Cp'_2Nb(Cl)(PMe_3)$,[39f] in reactions involving the displacement of the carbonyl or phosphine ligands; the carbonyl reaction exhibited 50% conversion after 12 h, while the phosphine displacement went to

(41) (a) Bellamy, A. J. *Anal. Chem.* **1980**, *52*, 607−608. (b) Marrese, C. A. *Anal. Chem.* **1987**, *59*, 217−218.

(42) (a) Abel, E. W.; Dansfer, M. O.; Waters, A. *J. Organomet. Chem.* **1973**, *49*, 287−321. (b) Roskamp, E. J.; Pedersen, S. F. *J. Am. Chem. Soc.* **1987**, *109*, 6551−6553. (c) Hartung, J. B., Jr.; Pedersen, S. F. *J. Am. Chem. Soc.* **1989**, *111*, 5468−5469.

(43) The broadening is due to unresolved coupling to neighboring Cp′ protons.

(44) For a detailed description of crystallographic techniques employed, see: Huffman, J. C.; Lewis, L. N.; Caulton, K. G. *Inorg. Chem.* **1980**, *19*, 2755−2762.

completion in this time. Since the process in eq 2 involves one less step and gives acceptable yields, this constitutes the preferred synthetic route. Compound **2** is the first isolated niobium compound containing an aldehyde or ketone ligand, and it should also be noted that similar reactions involving acetaldehyde, benzaldehyde, or acetone all failed to generate isolable adducts.

Compound **2** exhibited spectral data consistent with the formulation given in eq 2. It showed four Cp′ resonances due to the equivalent Cp′ ligands, requiring a plane of symmetry containing the Nb, Cl, C, and O atoms. The formaldehyde ligand gave rise to a proton resonance at 3.37 ppm and a ^{13}C resonance at 67.8 ppm (C_6D_6); both of these values are upfield of those for free aldehydes. In addition, the formaldehyde ligand stretching frequency (ν_{CO}) showed at 1179 cm^{-1}. All of these data suggest the η^2 formulation, for which typical stretching frequencies range from 1000 to 1200 cm^{-1}.[4a] Conversely, η^1 carbonyls show downfield NMR resonances and higher energy C−O stretching frequencies (ca. 1550 cm^{-1}) more reminiscent of the free aldehyde.[4a] These solution data are also consistent with the solid-state structure, which is discussed below.

Reactivity of 2. A brief survey showed that **2** is relatively inert toward other potential ligands. It failed to react with excess PMe_3 or 1 atm of CO, even after 1 day at ambient temperature. This is consistent with the alternative synthetic routes noted above, in which formaldehyde displaced both of these ligands. It also contrasts the chemistry of the vanadocene analogue $Cp_2V(\eta^2\text{-}CH_2O)$, from which the formaldehyde ligand is readily displaced by CO.[6b] Conversely, **2** is considerably more sensitive to oxidation than are the ketene complexes we have reported.[38] It decomposed rapidly in air to give the known oxide $Cp'_2Nb(Cl)(=O)$[39f] and slowly in chloroform solution to give the known Cp'_2NbCl_2;[45] there was no evidence for oxidation of the formaldehyde ligand in the former case, as we could detect no appreciable quantity of formic acid.

Finally, we treated **2** with MeLi in an effort to effect ligand exchange and/or insertion chemistry, but this led to decomposition of **2**. We subsequently determined that the desired compound was available from known $Cp'_2Nb(Me)(PMe_3)$,[39a] which reacted smoothly with excess paraformaldehyde to give $Cp'_2Nb(Me)(\eta^2\text{-}CH_2O)$. This derivative showed spectral properties similar to those of **2**, including an IR band at 1177 cm^{-1}. It is also air-sensitive, giving the known $Cp'_2Nb(Me)(=O)$[39f] upon exposure to oxygen.

Redox Routes to Hydride 4. The results described above established that **2** was relatively unreactive, and we were interested in other derivatives that might present more sites for chemical manipulation. In addition, we also sought to vary the oxidation state of the niobium center to create an empty coordination site. Both of these goals were realized in the preparation of hydride derivative $Cp'_2Nb(H)(\eta^2\text{-}CH_2O)$ (**4**). Treatment of **2** with amalgamated sodium gave rise to a pale green color and the ESR spectrum shown in Figure 1; this appears in either toluene or THF solution, but the use of toluene facilitates the ESR determination (it absorbs less microwave radiation than does THF). The signal

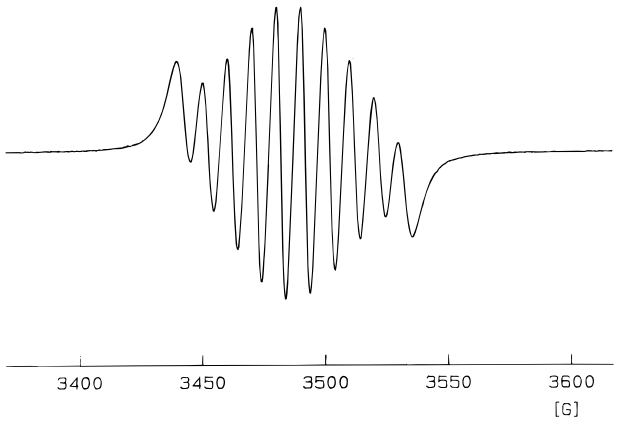

Figure 1. ESR spectrum of **3** in toluene solution.

consists of 10 lines and exhibits an isotropic g value of 2.003 and hyperfine splitting constant $\langle a \rangle = 10.30$ G. The splitting is due to the ^{93}Nb nucleus, which is 100% abundant and has nuclear spin $I = {}^9/_2$. We thus assign this signal to the Nb(IV) radical (**3**) depicted in eq 3.

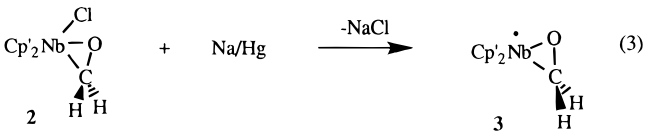

(3)

While $Cp_2Nb(IV)$ systems with two σ donor ligands often show $\langle a \rangle_{Nb}$ values of ca. 100 G,[45,46] low values are not uncommon for systems containing π-complexed ligands;[47a] this may be due to delocalization of unpaired spin density onto the ligand, but this explanation has been questioned.[47b] A solution infrared spectrum (toluene) of **3** contains a band at 1167 cm^{-1}, consistent with the retention of the formaldehyde ligand. Spectroscopic monitoring of the clear (homogeneous) reaction solution confirmed the loss of diamagnetic **2** (NMR) and the absence of any ESR-active species except **3**, so the redox reaction is apparently very clean. In addition, solutions of **3** were stable for lengthy periods when maintained under a nitrogen atmosphere. However, **3** was unstable toward isolation, giving rise at high concentrations (greater than ca. 2.5 mM) to two other compounds exhibiting 10-line ESR spectra with $\langle a \rangle$ values of ca. 95 and 100 G, respectively; it is difficult to assign g values or precise $\langle a \rangle$ values due to the overlap of the signals. We have not yet characterized these new products (which result from an undesirable side reaction from radical **3**), as they cannot be separated without decomposition and display no other useful spectroscopic handles. Thus, **3** may be generated quantitatively, is indefinitely stable in dilute solution, and fails to react with excess sodium amalgam. An analogue of **3**, $Cp'_2Nb(\eta^2\text{-}OCH\text{-}CHPh_2)$, has been reported in an electrochemical study, and it too was found unstable toward isolation.[47a]

If the reduction depicted in eq 3 was carried out using excess amalgam (minimum 2.5 equiv) and in the pres-

(45) Hitchcock, P. B.; Lappert, M. F.; Milne, C. R. C. *J. Chem. Soc., Dalton Trans.* **1981**, 180−186.

(46) Manzer, L. E. *Inorg. Chem.* **1977**, *16*, 525−528. (b) Broussier, R.; Normand, H.; Gautheron, B. *J. Organomet. Chem.* **1978**, *155*, 337−346. (c) Al-Mowali, A.; Kuder, W. A. A. *J. Organomet. Chem.* **1980**, *194*, 61−68. (d) Bottomley, F.; Keizer, P. N.; White, P. S.; Preston, K. F. *Organometallics* **1990**, *9*, 1916−1925.

(47) (a) Lucas, D.; Chollet, H.; Mugnier, Y.; Antiñolo, A.; Otero, A.; Fajardo, M. *J. Organomet. Chem.* **1992**, *426*, C4−C7. (b) Antiñolo, A.; Fajardo, M.; de Jesus, E.; Mugnier, Y.; Otero, A. *J. Organomet. Chem.* **1994**, *470*, 127−130.

ence of added methanol or ethanol, the result was the diamagnetic hydride **4** (eq 4). We also pursued the use

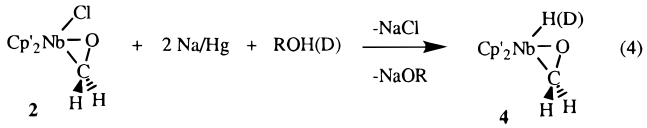

(4)

of other synthetic approaches to this compound; these involved (a) the reaction of Cp'_2NbH_3 with excess paraformaldehyde and (b) the reaction of formaldehyde chloride **2** with hydride sources such as $LiAlH(O^iBu)_3$. In both cases we observed general decomposition of the niobium starting material, with no evidence for the formation of **4**; hence, the route in eq 4 constitutes the only successful approach. The hydride ligand in **4** was evident from the ^1H NMR resonance at 0.69 ppm and from a broad IR band at 1697 cm^{-1}, while the formaldehyde ligand exhibited NMR signals at 2.30 ppm (proton) and 44.6 ppm (carbon) and an IR band at 1171 cm^{-1}. Compound **4** may be obtained as an off-white solid free from paramagnetic impurities, and this was facilitated by the prompt addition of the alcohol. Since synthetic reactions are normally run at concentrations higher than those used for spectroscopic monitoring, best synthetic results were obtained by adding a solution of **2** and excess alcohol directly to an excess (15 equiv) of the amalgam; this gave full conversion while avoiding the production of the unwanted paramagnetic side products mentioned above. Nonetheless, we have verified that radical **3** is on the path to hydride **4** by first generating dilute solutions of **3** as in eq 3 and then carrying **3** on to **4** with alcohol and a second 1 equiv of sodium. This is obviously a redox process as well, and **3** does not yield **4** in the absence of reductant. In addition, we have verified that the alcohol is the source of the hydride ligand in **4**; the use of CH_3OD gave **3**-d_1 (eq 4) with ≥95% D incorporation (by ^1H NMR), and deuterium was found only in the indicated position (by ^2H NMR). The conversion of **3** to **4** formally involves the addition of a hydrogen atom. Other metal-centered radicals have been seen to react with hydrogen atom sources such as $(n\text{-}Bu)_3SnH$,[48] which was thus added to a solution of **3**. A reaction ensued, but there was no evidence of **4**; the result was another Nb(IV) product (by ESR), the identity of which remains unknown.

Inasmuch as sodium amalgam has sufficient reducing power to reduce alcohols to alkoxide and H_2 (albeit slowly), we performed mechanistic studies to determine if H_2 was the active agent in the conversion of **3** to **4**. As such, radical **3** was generated with the addition of excess sodium amalgam (5 equiv). The solution of **3** was then removed from the amalgam, the flask evacuated, and 1 atm of H_2 admitted. In this way the partial pressure of H_2 established was far in excess of that produced by the slow action of sodium amalgam on alcohol. In fact, this reaction with H_2 produced only traces of **4**, and the major product was instead the oxomethyl derivative[39f] (eq 5). Hence, the production of **4** does not involve a reaction with H_2 (a mechanistic discussion follows below), but H_2 is apparently capable of cleaving the C−O bond in the formaldehyde ligand.

The mechanism of this latter process is not clear and may involve prior M−C hydrogenolysis to a methoxide

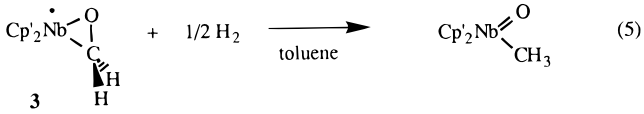

(5)

complex;[20] we attempted to enter this reactivity manifold with **1** and methoxide salts, but this led only to decomposition of **1**.

Voltammetric Data. We initiated voltammetric studies to gather mechanistic information regarding the reduction of **2**. The cathodic voltammetry was carried out in THF solution so as to match the synthetic system; the relatively low conductivity of THF necessitates the use of large concentrations of electrolyte, so the solutions contained 0.5 M $NBu_4^+PF_6^-$ and 2 mM concentrations of **2**. The system consisted of a mercury-coated platinum disk working electrode,[41] platinum wire counter electrode, and $Ag/AgNO_3$ reference electrode; all potentials are thus relative to the $Ag/AgNO_3$ couple, which is ca. 0.35 V positive of the standard calomel electrode (SCE) system. The resulting redox behavior is shown in Figure 2, which contains voltammograms for **2** in the presence of varying amounts of ethanol; the ethanol concentrations range from 0.054 M (Figure 2a) to 0.19 M (Figure 2c), with the latter representing a 95-fold excess of ethanol relative to **2**. It is clear that there is a reduction ocurring at $E_p = -2.32$ V vs $Ag/AgNO_3$, and there is no evidence for a corresponding anodic process on the return sweep, even if the switching potential is set at −2.5 V. Increasing alcohol concentration had no significant effect on the first wave at −2.32 V, the peak potential of which remained unchanged. The current of this peak rose slightly because the baseline rose with increasing alcohol concentration, doubtless due to an alcohol reduction wave outside the potential range probed. It is clear that these voltammograms also contain a reduction wave at −2.65 V and that its current increases with increasing ethanol concentration; this wave is absent prior to alcohol addition. At the same time, however, the current flowing at $E_p = -2.65$ V never equaled that of the cathodic wave at −2.32 V. A background voltammogram on a solution containing 0.19 M ethanol and 0.5 M $NBu_4^+PF_6^-$ electrolyte in THF tails up at the end of the sweep but is otherwise featureless; thus, the wave at −2.65 V is not due to reduction of ethanol or any unkown impurity in the ethanol. Indeed, the mercury-coated working electrode was specifically chosen to avoid unwanted alcohol reduction in the potential range studied, since mercury electrodes are known to require substantial overpotentials for hydrogen production.[49]

Discussion

Structure of 2. Some metal centers have been observed to form dimeric compounds with bridging formaldehyde ligands[6a,8,14] or to activate formaldehyde C−H bonds.[5,6a,50] To rule out the possibility that **2** was actually a formyl hydride undergoing rapid exchange, we sought crystallographic confirmation of the structure proposed for **2** in eq 2. Slow cooling of a saturated toluene solution of **2** to −30 °C led to the formation of

(48) Bruno, J. W.; Huffman, J. C.; Green, M. A.; Zubkowski, J. D.; Hatfield, W. E.; Caulton, K. G. *Organometallics* **1990**, *9*, 2556−2567.

(49) Galus, Z. In *Laboratory Techniques in Electroanalytical Chemistry*; Kissinger, P. T., Heineman, W. R., Eds.; Marcel Dekker: New York, 1984; Chapter 9.

(50) Thorn, D. L. *J. Am. Chem. Soc.* **1980**, *102*, 7109−7110.

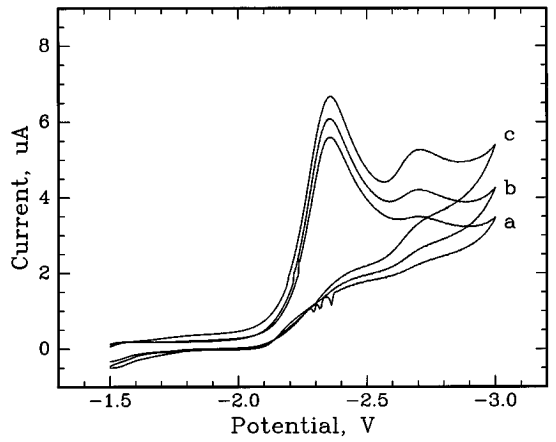

Figure 2. Cyclic voltammograms for compound **2** (2 mM) in THF (0.5 M $NBu_4^+PF_6^-$) containing (a) 0.054 M ethanol, (b) 0.10 M ethanol, and (c) 0.19 M ethanol. Sweep rates = 250 mV s^{-1}. The small spikes in the return sweep (at ca. −2.3 V) are instrumental artifacts.

pale yellow rods. These were found to diffract satisfactorily, and the resulting crystal data are shown in Table 1, key metrical parameters are given in Table 2, and full structural details are contained in the Supporting Information. The diffraction data were indicative of a disorder, and the final model is based on a crystal in which 9% of the sites were filled with **2** in an alternate orientation. In this model it appears that the minor component of **2** has been rotated about an axis approximately coinciding with the Nb−O bond, thereby interchanging the positions of the Nb−Cl and Nb−CH_2 moieties. The model does account for the observed data accurately; a final difference Fourier map was featureless and the fit with experimental data yielded $R(F)$ = 0.0404 and $R_w(F)$ = 0.0293. Because of the disorder problem and the low abundance of the minor crystal component, its structure could not be determined with confidence. We considered the possibility that the minor component resulted from a true structural isomer, but there was no spectral evidence for this; in particular, solid-state infrared spectroscopy showed no evidence for a η^1-formaldehyde complex.

The disorder problem could potentially impact the accuracy of the metrical parameters obtained for the major crystal component. However, we have considered these bond lengths and angles carefully and find them entirely within the ranges seen for related compounds. The resulting structure is presented in Figure 3, from which it is clear that solid-state **2** adopts the expected bent metallocene geometry with chloride and formaldehyde ligands in the equatorial plane. The formaldehyde hydrogens were located and refined, thereby distinguishing the carbon and oxygen atoms and verifying the O-inside disposition of the formaldehyde ligand. The Cp′ ligand parameters are typical, with Nb−C bond lengths ranging from 2.407(4) to 2.454(4) Å. The Nb−Cl bond length is 2.5253(11) Å, and this may be compared to literature data for other niobocene derivatives. Six other niobocene chlorides reported in the literature exhibit Nb−Cl bond lengths ranging from 2.450(10) to 2.538(2) Å for Nb(V) derivatives,[35f,36a,51−53]

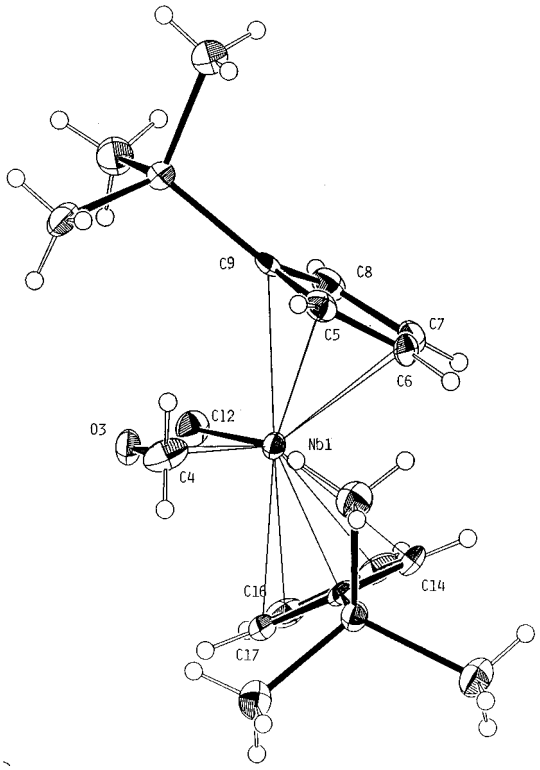

Figure 3. Structure of compound **2** showing the atom-numbering scheme.

so **2** is within this range. The Nb−C(4) bond length in **2** (2.257(4) Å) may be compared to the Nb−C bond lengths (Å) for a series of alkyl compounds, including $Cp_2Nb(C_2H_4)(Et)$ (2.316(8)),[54] $[Cp_2Nb(^nBu)]_2O$ (2.32(1)),[55] and $Cp_2Nb(O)(Me)$ (2.221(21)).[39f] For π-complexed carbon ligands the Nb−C bond lengths vary as indicated for the series $Cp'_2Nb(Cl)(\eta^2$-PhCCPh) (2.171(8), 2.185(9)),[39a] $(C_5H_4Me)_2Nb(\eta^2$-$CO_2)(CH_2SiMe_3)$ (2.144(7)),[56] $Cp'_2Nb(Cl)(\eta^2$-*C*,*N*-PhN=C=PMes) (2.198(17)),[53] $Cp_2Nb(C_2H_4)(Et)$ (2.320(9), 2.277(9)),[54] and $Cp^*_2Nb(H)(PhCH{=}CH_2)$ (2.309(4), 2.289(4)).[57] Hence the value for **2** falls well within the ranges of 2.221(21)−2.32(1) for alkyls and 2.144(7)−2.320(9) Å for η^2-bound carbon-containing ligands. The structural data for the formaldehyde ligand in **2** are also similar to those seen for other aldehyde complexes. The C−O bond length of 1.322(5) Å is comparable to those (in Å) seen for $Cp_2V(CH_2O)$ (1.353(10)),[6b] $Fe(CO)_2(P(OMe)_3)_2(CH_2O)$ (1.32(2)),[9] $W(PMe_3)_2(S)_2(PhCHO)$ (1.376(9)),[17] and a series of rhenium complexes of general formula $[CpRe(NO)(PPh_3)(RCHO)][PF_6]$ (R = H, 1.374(19); R = Et, 1.35(1); R = Bz, 1.318(11); R = *n*-Pr, 1.338(5)).[58] Only the osmium complex $Os(PPh_3)_2(CO)_2(CH_2O)$ falls outside of this range, with an abnormally long C−O bond (1.59(1) Å) and a very low C−O stretching frequency (1017 cm^{-1}).[5]

(51) Bkouche-Waksman, I.; Bois, C.; Sala-Pala, J.; Guerchais, J. E. *J. Organomet. Chem.* **1980**, *195*, 307−315.
(52) Chernega, A. N.; Green, M. L. H.; Suarez, A. G. *J. Chem. Soc., Dalton Trans.* **1993**, 3031−3034.
(53) Alexander, J. B.; Glueck, D. S.; Yap, G. P. A.; Rheingold, A. L. *Organometallics* **1995**, *14*, 3603−3606.
(54) Guggenberger, L. W.; Meakin, P.; Tebbe, F. N. *J. Am. Chem. Soc.* **1974**, *96*, 5420−7.
(55) Kirillova, N. I.; Lemenovskii, D. A.; Baukova, T. V.; Struchkov, Yu. T. *Koord. Khim.* **1978**, *3*, 1254−1260.
(56) Bristow, G. S.; Hitchcock, P. B.; Lappert, M. F. *J. Chem. Soc., Chem. Commun.* **1981**, 1145−1146.
(57) Burger, B. J.; Santarsiero, B. D.; Trimmer, M. S.; Bercaw, J. E. *J. Am. Chem. Soc.* **1988**, *110*, 3134−3146.
(58) Klein, D. P.; Méndez, N. Q.; Seyler, J. W.; Arif, A. M.; Gladysz, J. A. *J. Organomet. Chem.* **1993**, *450*, 157−164.

Hence, there was no indication that the disorder in the crystal of **2** resulted in any distortion of the metrical parameters calculated for the major crystal component. As such, it is also worth considering the disposition of the metal center along the C−O vector. Gladysz has defined a slip parameter indicating the degree to which the metal center moves from the center of the C−O bond toward the oxygen terminus, and this is expressed as a percentage of half the C−O bond length (the distance from the midpoint to the termini);[58] a similar parameter has previously been determined for alkene complexes.[59] The cationic rhenium formaldehyde complex exhibits 16% slippage,[60] $Cp_2V(CH_2O)$ shows 30% slippage,[6b] and $Fe(CO)_2(P(OMe)_3)_2(CH_2O)$ slips 7%;[9] for **2** this value is 51%, indicating considerable slip toward the oxygen terminus. Since the oxygen is located in the endo (inside) position, we determined the inherent contribution of niobocene endo/exo binding differences by calculating the slip for the symmetrical ligands found in $Cp_2Nb(\eta^2\text{-}O_2)(Cl)$,[51] $Cp_2Nb(\eta^2\text{-}C_2H_4)(Et)$,[54] and $Cp'_2Nb(\eta^2\text{-}PhCCPh)(Cl)$;[39a] these indicated only a modest slip toward the endo terminus, with values of 6%, 9%, and 3%, respectively. Hence, the oxophilic character of the niobium center in **2** leads to a substantial slip toward the oxygen terminus of the ligand.

Mechanistic Considerations. The introduction of the hydride ligand in **4** could be envisioned to involve any of three discrete mechanistic paths; these require reduction of **3**, and they differ with respect to the site of protonation (C, O, or Nb, respectively) of the resulting anion. The first two of these processes would proceed via the intermediacy of **C** or **D**. We will first consider

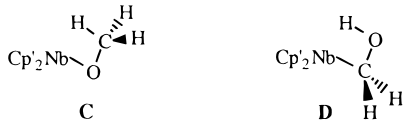

C **D**

this regiochemical question and then return to a consideration of the role of alcohol in the initial production of the anion. On the basis of literature precedent, the most likely path for formation of **3** is that involving β-hydride elimination from an intermediate methoxide (**C**).[20−37] Indeed, we have invoked a similar pathway in our ketene complexes, which are proposed to form hydrides via the route shown in eq 6;[38c] the intermediate

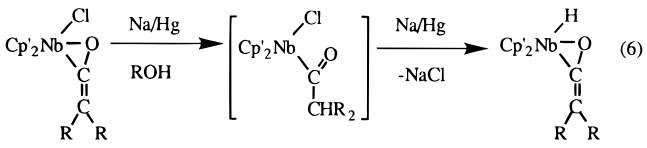

(6)

acyl results from reduction and protonation of the ketene ligand, and then undergoes β-H elimination after reductive loss of chloride. We have corroborated this claim with deuterium labeling studies and alternate preparation of the proposed intermediate acyl. However, we can eliminate a related mechanism for formaldehyde complex **2** on the basis of a few experimental observations. First, the added alcohol cannot be the source of an alkoxide; we observed only **4**, regardless of the alcohol (e.g., ethanol or methanol) used. Also, we can discount the notion that the formaldehyde ligand in **2** was converted to alkoxide via a sequence involving reduction and protonation on carbon. Our use of MeOD showed that deuterium was incorporated into **4** only at the Nb−H(D) site. A hypothetical intermediate containing a $Nb-OCH_2D$ moiety would certainly undergo a combination of β-H and β-D eliminations, yielding a mixture of $Nb(D)(OCH_2)$ and $Nb(H)(OCHD)$ isotopomers; none of the latter was observed by ^2H NMR. Hence, a mechanism involving intermediate **C** is not operative.

The remaining possibilities are more difficult to distinguish. Here the second reduction product is subsequently protonated by alcohol on O or Nb, respectively. Reasonable precedents exist for either path; electron-rich formaldehyde complexes often add electrophiles at oxygen,[1,6,8,9,14,60] and intermediate **D** would arise from protonation at the formaldehyde oxygen. In addition, Cp_2NbH_3 and Cp_2MH_2 (M = Mo, W) can be deprotonated with sodium hydride or lithium alkyls, and the resulting anions can be protonated readily (presumably on the metal center);[61] this is analogous to our proposal for protonation at the niobium center, involving the direct formation of **4**. While both paths are conceivable, we must also consider the nature of the anionic intermediate and the route by which it is formed. We noted that radical **3** may be stirred over excess sodium amalgam for lengthy periods, during which NMR and ESR show no evidence of any reaction. Clearly, however, the subsequent reactivity of **3** must be redox-induced, since it fails to yield **4** with either H_2 or alcohol in the absence of sodium. This situation is reminiscent of the mechanistic discussions regarding dissolving metal reductions of aldehydes and ketones to alcohols (eq 7).[62−66] These processes may occur in liquid ammonia

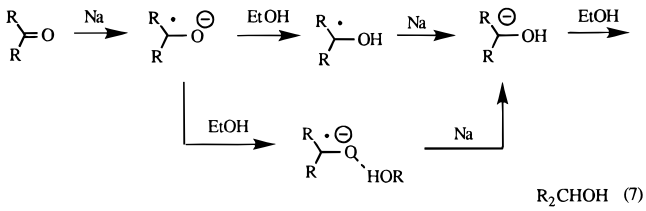

R_2CHOH (7)

or in alcohols (Bouveault−Blanc procedure), and there is considerable disagreement regarding the operation of electron, electron, proton (e^-, e^-, H^+) or electron,

(59) (a) Eisenstein, O.; Hoffmann, R. *J. Am. Chem. Soc.* **1981**, *103*, 4308−4320. (b) Cameron, A. D.; Smith, V. H., Jr.; Baird, M. C. *J. Chem. Soc., Dalton Trans.* **1988**, 1037−1043.

(60) (a) Bendix, M.; Grehl, M.; Frohlich, R.; Erker, G. *Organometallics* **1994**, *13*, 3366−3369. (b) Gibson, D. H.; Franco, J. O.; Sleadd, B. A.; Naing, W.; Mashuta, M. S.; Richardson, J. F. *Organometallics* **1994**, *13*, 4570−4577. (c) Ashkam, F. R.; Carroll, K. M.; Briggs, P. M.; Rheingold, A. L.; Haggerty, B. S. *Organometallics* **1994**, *13*, 2139−2141. (d) Erker, G.; Bendix, M.; Petrenz, R. *Organometallics* **1994**, *13*, 456−461.

(61) (a) Francis, B. R.; Green, M. L. H.; Luong-thi, T.; Moser, G. A. *J. Chem. Soc., Dalton Trans.* **1976**, 1339−1345. (b) Lemenovskii, D. A.; Nifant'ev, I. E.; Urazowski, I. F.; Perevalova, E. G.; Timofeeva, T. V.; Slovokhotov, Yu. L.; Struchkov, Yu.T. *J. Organomet. Chem.* **1988**, *342*, 31−44. (c) Green, M. L. H.; Hughes, A. K.; Mountford, P. *J. Chem. Soc., Dalton Trans.* **1991**, 1699−1704.

(62) (a) Huffman, J. W. *Acc. Chem. Res.* **1983**, *16*, 399−405. (b) Huffman, J. W.; Liao, W.-P.; Wallace, R. H. *Tetrahedron Lett.* **1987**, *28*, 3315−3318.

(63) Pradhan, S. K. *Tetrahedron* **1986**, *42*, 6351−6388.

(64) (a) Rautenstrauch, V. *Tetrahedron* **1988**, *44*, 1613−1618. (b) Rautenstrauch, V.; Geoffroy, M. *J. Am. Chem. Soc.* **1976**, *98*, 5035−5037. (c) Rautenstrauch, V.; Geoffroy, M. *J. Am. Chem. Soc.* **1977**, *99*, 6280−6286.

(65) Giordano, C.; Perdoncin, G.; Castaldi, G. *Angew. Chem., Int. Ed. Engl.* **1985**, *24*, 499−500.

(66) Song, W. M.; Dewald, R. R. *J. Chem. Soc., Perkin Trans. 2* **1989**, 269−273.

proton, electron (e^-, H^+, e^-) sequences leading to alkoxide. Electrochemical studies on ketones and aldehydes have been invoked to show that sodium metal does not have sufficient reducing power to produce the carbonyl dianions,[62] and this has been cited as evidence favoring the e^-, H^+, e^- route (eq 7, top). However, it has also been suggested that the alternative e^-, e^-, H^+ sequence is facilitated by hydrogen bonding effects (eq 7, bottom; ion-pairing with Na^+ is operative in both pathways and is omitted for clarity), such that the second reduction is rendered thermodynamically accessible and is essentially coupled with proton transfer.[63] A recent stopped-flow kinetic study also suggests that the e^-, e^-, H^+ route may be operative; there is evidence for a second-order kinetic dependence on reductant and no kinetic contribution from added alcohol cosolvents.[66] These observations have been corroborated by Houk in a recent theoretical study,[67] in which it is suggested that the second reduction event may indeed be aided by hydrogen-bond donation by the alcohol solvent. The reaction involving conversion of **2** to **4** (eq 4) is an organometallic version of the sodium/alcohol reduction and is similar to the Bouveault−Blanc procedure in that (a) it provides access to reduction products that are not available with the use of hydridic reductants and (b) it requires the presence of alcohol to facilitate the second reduction event. Although there is no experimental evidence for hydrogen-bond assistance in the Bouveault−Blanc process, our voltammetric data constitute evidence for such a process in the reduction of **2**.

Voltammetry. The second reduction wave at $E_p = -2.65$ V (Figure 2) does not depend in a simple way on ethanol concentration, but it does show evidence for an anodic wave on the return sweep; it thus originates from a quasi-reversible process. We believe that the voltammetric behavior is best described by the sequence depicted in Scheme 1. Here we see the wave at −2.32 V resulting from reduction and prompt loss of chloride, a process that has been seen for a number of other early transition metal chlorides;[68] this is consistent with the irreversible nature of the first voltammetric redox process as well as our direct observation of **3** in the synthetic work, and neutral **3** should be much more difficult to oxidize than would be the hypothetical $\mathbf{2}^-$. We then invoke an equilibrium process involving hydrogen bonding of the alcohol to the **3** produced at −2.32 V, such that the hydrogen-bonded species (**5**) is responsible for the wave at −2.65 V; steps 10 and 11 thus constitute a CE process for reduction of **3**. This is more likely than an EC process in which an endothermic reduction is driven by a subsequent protonation. The Nernst equation would dictate that the reduction potential in an EC process would shift to less negative potentials with increasing alcohol concentration, but the potential of the second reduction wave is constant for widely different alcohol concentrations. The first reduction wave is entirely unaffected by added ethanol, so there is no evidence for any role for ethanol in the reduction of **2** (eqs 8 and 9). The equilibrium between **3** and ethanol is clearly an unfavorable one, since very large excesses of ethanol convert less than ca. 30% of the **3** at the electrode to **5** (as estimated from the relative currents represented in the two waves in Figure 2c). The proposed equilibrium process for the formation of **5** is reasonable, since it constitutes another example of Lewis acid activation of a formaldehyde ligand. The Nb(IV) species **3** should be more electron-rich than the Nb(V) precursor **2** and, hence, more susceptible to activation by a weak Lewis acid. Moreover, our synthetic studies show that **3** does not undergo any irreversible reaction with alcohol, so this cannot be the cause of the wave at −2.65 V. We thus attribute the second reduction wave to the complex **5**, which then ejects alkoxide. The resulting species **6** is the direct precursor to **4** and is depicted as an open hydroxymethyl compound. In fact, **6** could preserve the Nb−O linkage and still transfer the hydrogen to the metal center; such a structure would be highly reminiscent of one postulated by Shriver for the product of protonation of $[HFe_4(CO)_{13}]^-$; the resulting $(\mu\text{-H})Fe_4(CO)_{13}(\mu^2\text{-COH})$ contained an η^2-hydroxycarbyne and ultimately gave the parent carbyne (CH) ligand upon further reduction.[69]

As an adjunct to these voltammetric studies, we attempted to observe the hydrogen-bonding equilibrium directly. We thus utilized ESR spectroscopy to study **3** (in toluene solution) as a function of added ethanol. A 0.9 mM solution of **3** in toluene was generated (as in eq 3), and the presence of **3** was confirmed with ESR; this exhibited the spectrum given in Figure 1. Next, 0.2 M ethanol was added to this solution, whereupon the ESR spectrum showed a slight decrease in the value of $\langle a \rangle_{Nb}$. This trend continued with increasing ethanol concentration until the sample exhibited a hyperfine splitting of 9.65 G (at 0.4 M ethanol), decreased from the 10.30 G splitting of **3** in pure toluene; the *g* value was also

Scheme 1

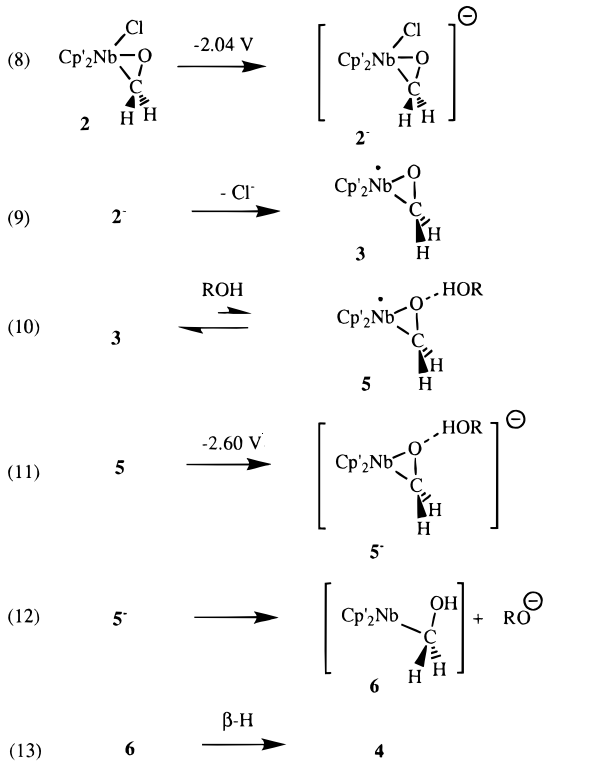

(67) Wu, Y.-D.; Houk, K. N. *J. Am. Chem. Soc.* **1992**, *114*, 1656−1661.

(68) (a) Chivers, T.; Ibrahim, E. D. *Can. J. Chem.* **1973**, *51*, 815−820. (b) Gubin, S. P.; Smirnova, S. A. *J. Organomet. Chem.* **1969**, *20*, 229−240. (c) Mugnier, Y.; Moise, C.; Laviron, E. *J. Organomet. Chem.* **1981**, *204*, 61−66. (d) Kotz, J. C. In *Topics in Organic Electrochemistry*; Fry, A. J., Britton, W. E., Eds.; Plenum: New York, 1986; Chapter 3.

(69) Whitmire, K. H.; Shriver, D. F. *J. Am. Chem. Soc.* **1981**, *103*, 6754−6755.

affected, increasing to 2.097 (vs 2.003 in pure toluene). These changes in g and $\langle a \rangle_{Nb}$ are sufficiently small that we considered other possible causes related to small changes in bulk solvent properties induced by the ethanol addition. Ethanol has a dielectric constant (24.55) and dipole moment (1.66 D) widely different from those of toluene (2.379, 0.31 D, respectively).[70] As such, identical toluene solutions of **3** were also titrated with similar concentrations of acetone ($\epsilon = 20.70$, $\mu = 2.69$ D) and pyridine ($\epsilon = 12.40$, $\mu = 2.37$ D);[70] neither of these had any effect on the ESR spectra of **3**, which were superimposible on the spectrum obtained in pure toluene. The spectrum of **3** was changed by addition of a small amount of ethanol, and this change was fully reproducible (three trials on separate solutions exhibited identical behavior). The spectrum is not sensitive to changes in bulk solvent properties (at the concentrations employed here), and ethanol is the only titrant of the three capable of hydrogen-bond donation; hence, we propose that the data described here are the result of the equilibrium in eq 10. We expect to see only the time-averaged spectrum resulting from equilibrating **3** and **5** (eq 10), and other systems have exhibited time-averaged ESR spectra for proton transfer processes.[71] Moreover, since the equilibrium is presumably an unfavorable one (see below), the solution will only contain small amounts of **5** under any conditions; hence, while we do not know the limiting ESR parameters for **5**, they would have to be very different from those of **3** to lead to large changes in the time-averaged ESR spectrum.

A reviewer has suggested an alternate formulation for hydrogen-bonded species **5**, in which the hydrogen-bonding interaction occurs between the alcohol and the metal center. Our data are not inconsistent with this scenario, which would lead directly from the isomeric $\mathbf{5}^-$ to product by way of fast expulsion of alkoxide (i.e., without the intervention of **6**). While 17 electron species such as **3** are indeed susceptible to association of an additional ligand, the latter usually donate an electron pair to generate a 19 electron transient. It is less clear that a hydrogen-bonding interaction could involve only the single electron on the metal center, since the incoming group (alcohol in this case) would be an electrophile (hydrogen-bond donor). Since the ESR effects noted above are only apparent for alcohol and not for other potential ligands, and since there are electron pairs available on the formaldehyde oxygen, we favor this as the site of hydrogen bonding.

Digital Simulations. In an attempt to establish the feasibility of the mechanism in Scheme 1 and to extract more information regarding individual chemical steps, we have simulated the process as written (Figure 4). This was done using the DigiSim program,[72a] for which the simulation method has recently been described.[72b] We first used the program to generate a fit to the experimental data, based on the mechanism shown in Scheme 1. This process was rendered somewhat difficult by the fact that we are operating near the cathodic edge of our available window. In particular, the tailing exhibited by the voltammograms is due to a combination of solvent breakdown and alcohol reduction, with the latter making the major contribution. Since we are using such large quantities of alcohol, we avoided scanning through the alcohol reduction wave. This naturally made the simulation of this wave difficult, since there is no experimental data for most of the wave under consideration; we do not claim even semiquantitative accuracy for that part of the redox mechanism. Nonetheless, we have included alcohol reduction as part of the simulation in an attempt to model the rise in the current as the potential approaches −3 V; the inaccuracy associated with this part of the simulated mechanism results in some divergence between simulation and experiment, but this is largely localized in cathodic end of the voltammograms. After generating approximate voltammetric parameters from the optimization, we refined these in subsequent simulations to approach the experimental data. In spite of the complications noted above, the simulations provide a reasonable model for the experimental data; the family of simulated voltammograms (Figure 4) may be compared with the experimental voltammograms in Figure 2. The simulated voltammograms a−c (Figure 4) differ only in the concentration of alcohol present, and all other parameters are unchanged. The ability of the model to match *three* experiments affords some confidence that the simulation parameters are a true representation of the experimental system and not a collection of spurious data that happens to reproduce one experimental result. A discussion of the simulation results follows; full details are given as Supporting Information.

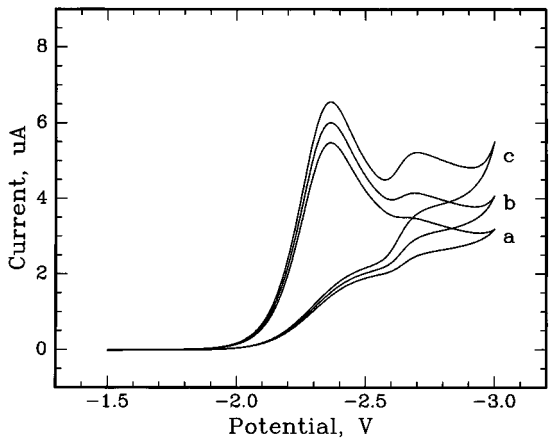

Figure 4. Simulated voltammograms generated with the DigiSim program. Conditions match those used for the experiments in Figure 2. Simulation details are discussed in the text and Supporting Information.

The optimized simulation has afforded values for the electrochemical and chemical steps depicted in Scheme 1, and we have carried out many additional simulations to determine the sensitivity of the fit to variations in the individual parameters. The first mechanistic step (eq 8) is an electrochemical one, and this process gives rise to the wave with $E_p = -2.32$ V. The thermodynamic potential for this step is −2.04 V, and the heterogeneous electron transfer rate is slow ($k_8 = 1.5 \pm 0.3 \times 10^{-3}$ cm s^{-1}). This latter observation and the

(70) Riddick, J. A.; Bunger, W. B. *Organic Solvents. Physical Properties and Methods of Purification*, 3rd ed.; Wiley-Interscience: New York, 1970.

(71) Wertz, J. E.; Bolton, J. E. *Electron Spin Resonance; Elementary Theory and Practical Applications*; Chapman and Hall: New York, 1986; Chapter 9.

(72) (a) Rudolph, M.; Feldberg, S. W. Available from Bioanalytical Systems, Inc., 2701 Kent Ave, W. Lafeyette, IN 47906. (b) Rudolph, M. In *Physical Electrochemistry, Principles, Methods and Applications*; Rubinstein, I., Ed.; Marcel Dekker, Inc.: New York, 1995; Chapter 3.

optimized value of the transfer coefficient ($\alpha = 0.375 \pm 0.010$) are consistent with some structural change accompanying the slow electron transfer, and this is the cause of the broadness exhibited in this wave. The nature of this chemical step is undoubtedly chloride loss (eq 9), as noted above. Our simulations indicate that this process is rapid and efficient, with large optimized values of k_9 (5×10^8 s^{-1}) and K_{eq} (2630 mol L^{-1}). In fact, however, the voltammograms are not very sensitive to the exact values for these parameters, as long as they satisfy the inequalities $K_{eq} > 200$ mol L^{-1} and $k_9 > 100$ s^{-1}. Saveant has established that the rate of halide loss following reduction of organic halides varies with the strength of the R−X bond and with the reduction potential (E_0);[73] these unimolecular reactions may be extremely fast, with, e.g., $k = 5 \times 10^7$ s^{-1} for chloride loss from the radical anion of 1-chloronapthalene. We are unaware of quantitive rate data for metal halides, and it may be that our simulated value is of the proper magnitude; in any case, it is clear that the voltammetric data are indicative of prompt and efficient loss of halide following reduction.

The simulations are quite sensitive to the rate and equilibrium constants for formation of hydrogen-bonded complex **5** (eq 10), as these parameters determine the size (height and breadth) of the second wave. The optimized values for this bimolecular chemical process (in the forward direction) are $k_{10} = 50 \pm 10$ L mol^{-1} s^{-1} and $K_{eq} = 0.08 \pm 0.01$ L mol^{-1}. However, the dependence on the electrochemical parameters (eq 11) is less stringent, with ranges $0.1 < k_{11} < 0.5$ cm s^{-1} and $0.15 < \alpha < 0.45$ giving acceptable fits.[74] Following this reduction, the resulting anion **5**$^-$ expels the alkoxide. This is again a rapid and efficient process ($k_{12} = 25 \pm 10$ s^{-1} and $K_{eq} = 2.5$ L mol^{-1}) as modeled. The quasi-reversible nature of the second redox wave indicates that **5**$^-$ has a finite lifetime and that methoxide ejection is not concurrent with reduction, and attempts to model the electrochemical process as wholly reversible ($k_{12} = 0$) or irreversible ($k_{12} \geq 10^6$ s^{-1}) do not reproduce (or even approach) the experimental voltammograms. The importance of the hydrogen-bonding interaction in facilitating the redox chemistry strongly implicates the mechanistic path involving direct protonation on the formaldehyde oxygen. This is also consistent with previous studies showing that heteroatom-containing ligands (e.g., carbonyls, nitrosyls, etc.) are inevitably the site of kinetic protonation;[75] in at least some cases this ligand-protonated species has been verified to lie on the path to the ultimate metal hydride.[75g,h] Hydroxymethyl compound **6** would yield **3** by β-hydride elimination. This occurs after the redox events and has no effect on the simulations. It should also be noted that acceptable simulations result from a model in which eq 12 (Scheme 1) involves protonation (directly on the niobium center) of **5**$^-$ by another alcohol. Our fitting procedures do not distinguish this bimolecular process from the unimolecular process depicted because we are operating under pseudo-first-order conditions; the large excess of alcohol is necessary to drive the poor equilibrium in eq 10. Hence, while our results do not eliminate direct metal protonation from consideration, they provide strong evidence for the hydrogen-bonding phenomenon.

Conclusions. Although not highly susceptible to coordination of alkenes or carbonyl compounds, **1** does exhibit especially strong binding of formaldehyde. The structural data are consistent with slippage of the metal center toward the oxygen terminus, but this is not reflected in the reactivity of **2**. We have succeeded in enhancing the reactivity of the niobocene−formaldehyde system using redox approaches. These can be manipulated to yield either paramagnetic **3** by way of a single-electron reduction path or metal hydride **4** by way of a two-electron reduction path. This latter reaction does not involve β-hydride elimination from an intermediate methoxide or reaction with dihydrogen. While the regiochemistry of protonation (O or Nb) is not established unequivocally, we have presented direct evidence for hydrogen-bond assistance in the second redox event; the latter does not occur in the absence of added alcohol, and we have voltammetric and ESR evidence showing that formation of the key redox intermediate requires both alcohol and initial product **3**. The importance of hydrogen bonding in organometallic systems has been the subject of several recent reports.[76] These effects have been identified in the solid state structures of several species,[76d,e] they have been observed in inert-gas solutions containing metal carbonyls and alcohols,[76j−n] and there is direct evidence for intramolecular interactions involving iridium hydride acceptors and heteroatom ligand (with N−H or O−H) donors.[76a,f−h] The

(73) (a) Saveant, J.-M. *J. Phys. Chem.* **1994**, *98*, 3716−3724. (b) Saveant, J.-M. *Acc. Chem. Res.* **1993**, *26*, 455−461. (c) Saveant, J.-M. *J. Am. Chem. Soc.* **1992**, *114*, 10595−10602 and references therein. (d) Saveant, J.-M. *Tetrahedron* **1994**, *50*, 10117−10165. (e) Adcock, W.; Andrieux, C. P.; Clark, C. I.; Neudeck, A.; Saveant, J.-M.; Tardy, C. *J. Am. Chem. Soc.* **1995**, *117*, 8285−8286. See also: (f) Lawless, J. G.; Bartak, D. E.; Hawley, M. D. *J. Am. Chem. Soc.* **1969**, *91*, 7121−7127.

(74) Other simulations have exhibited weak dependence on some of the electrochemical parameters: Richards, T. C.; Geiger, W. E.; Baird, M. C. *Organometallics* **1994**, *13*, 4494−4500.

(75) (a) Hodali, H. A.; Shriver, D. F.; Ammlung, C. A. *J. Am. Chem. Soc.* **1978**, *100*, 5239−5240. (b) Fachinetti, G. *J. Chem. Soc., Chem. Commun.* **1979**, 397−398. (c) Keister, J. B. *J. Organomet. Chem.* **1980**, *190*, C36−C38. (d) Stevens, R. E.; Goettler, R. D.; Gladfelter, W. L. *Inorg. Chem.* **1990**, *29*, 451−456. (e) Stevens, R. E.; Gladfelter, W. L. *J. Am. Chem. Soc.* **1982**, *104*, 6454−6457. (f) Nevinger, J. R.; Keister, J. B.; Maher, J. *Organometallics* **1990**, *9*, 1900−1905. (g) Pribich, D. C.; Rosenberg, E. *Organometallics* **1988**, *7*, 1741−1745. (h) Rosenberg, E. *Polyhedron* **1989**, *8*, 383−405. (i) Krisjansdottir, S. S.; Norton, J. R. In *Transition Metal Hydrides: Recent Advances in Theory and Experiment*; Dedieu, A., Ed.; VCH: New York, 1992; Chapter 9. (j) Astruc, D. *Electron Transfer and Radical Processes in Transition-Metal Chemistry*; VCH: New York, 1995; Chapter 5.

(76) (a) Stevens, R. C.; Bau, R.; Milstein, D.; Blum, O.; Koetzle, T. F. *J. Chem. Soc., Dalton Trans.* **1990**, 1429−1432. (b) Orton, D. M.; Green, M. *J. Chem. Soc., Chem. Commun.* **1991**, 1612−1614. (c) Kirchner, K.; Mereiter, K.; Mauthner, K.; Schmid, R. *Organometallics* **1994**, *13*, 3405−3407. (d) Braga, D.; Grepioni, G.; Biradha, K.; Pedireddi, V. R.; Desiraju, G. R. *J. Am. Chem. Soc.* **1995**, *117*, 3156−3166. (e) Braga, D.; Grepioni, B.; Sabatino, P.; Desiraju, G. R. *Organometallics* **1994**, *13*, 3532−3543. (f) Lough, A. J.; Park, S.; Ramachandran, R.; Morris, R. H. *J. Am. Chem. Soc.* **1994**, *116*, 8356−8357. (g) Lee, J. C., Jr.; Peris, E.; Rheingold, A. L.; Crabtree, R. H. *J. Am. Chem. Soc.* **1994**, *116*, 11014−11019. (h) Peris, E.; Lee, J. C., Jr.; Rambo, J. R.; Eisenstein, O.; Crabtree, R. H. *J. Am. Chem. Soc.* **1995**, 117, 3485−3491. (i) Fairhurst, S. A.; Henderson, R. A.; Hughes, D. L.; Ibrahim, S. K.; Pickett, C. J. *J. Chem. Soc., Chem. Commun.* **1995**, 1569−1570. (j) Lokshin, B. V.; Kazarian, S. G.; Ginzburg, A. G. *J. Mol. Struct.* **1988**, *174*, 29−34. (k) Lokshin, B. V.; Ginzburg, A. G.; Kazarian, S. G. *J. Organomet. Chem.* **1990**, *397*, 203−208. (l) Lokshin, B. V.; Kazarian, S. G.; Ginzburg, A. G. *Izv. Akad. Nauk SSR, Ser. Khim.* **1986**, 2605−2608. (m) Lokshin, B. V.; Kazarian, S. G.; Ginzburg, A. G. *Izv. Akad. Nauk SSR, Ser. Khim.* **1987**, 948−951. (n) Lokshin, B. V.; Kazarian, S. G.; Ginzburg, A. G. *Izv. Akad. Nauk SSR, Ser. Khim.* **1988**, 333−338. (o) Hamley, P. A.; Kazarian, S. G.; Poliakoff, M. *Organometallics* **1994**, *13*, 1767−1774. (p) Brammer, L.; Zhao, D. *Organometallics* **1994**, *13*, 1545−1547. (q) Stang, P. J.; Cao, D. H.; Poulter, G. T.; Arif, A. M. *Organometallics* **1995**, *14*, 1110−1114. (r) Portnoy, M.; Milstein, D. *Organometallics* **1994**, *13*, 600−609. (s) Dyer, P. W.; Gibson, V. C.; Jeffery, J. C. *Polyhedron* **1995**, *14*, 3095−3098. (t) Peris, E.; Crabtree, R. H. *J. Chem. Soc., Chem. Commun.* **1995**, 2179−2180. (u) Kazarian, S. G.; Hamley, P. A.; Poliakoff, M. *J. Am. Chem. Soc.* **1993**, *115*, 9069−9079.

current work contains the most dramatic example (from the standpoint of subsequent chemical reactivity) of the influence of hydrogen-bond formation, since the reduction of **3** is impossible in its absence. This sodium−ethanol reaction constitutes the only synthetic route to hydride **4**, and the situation is reminiscent of the Bouveault−Blanc reaction, both mechanistically and synthetically.[62,63] The mechanism of the latter has proven difficult to establish unequivocally, but current evidence favors the intermediacy of a hydrogen-bonded complex involving alcohol and ketyl radical anion. The reaction has been seen to result in carbonyl reductions (e.g., stereochemical outcomes) that are inaccessible using metal hydride reductants, just as our organometallic application serves as the only viable route to **4**. We are currently probing the scope of this reaction.

Acknowledgment. We thank the National Science Foundation for financial support of this work and Professor Al Fry and Mr. John Porter for assistance with the electrochemical experiments.

Supporting Information Available: Crystal data for **2**, including a textual summary of the analysis, tables of crystal data, bond lengths and angles, atomic coordinates, and thermal parameters, and structure drawings, and output from DigiSim simulations (26 pages). Ordering information is given on any current masthead page.

OM960106W